Published in final edited form as:
Arch Oral Biol. 2013 September ; 58(9): 1148–1154. doi:10.1016/j.archoralbio.2013.03.001.

Effects of *Fam83h* Overexpression on Enamel and Dentin Formation

Young-Sun Kweon[1], **Kyung-Eun Lee**[1], **Jiyeon Ko**[1], **Jan C-C. Hu**[2], **James P. Simmer**[2], and **Jung-Wook Kim**[1,3]

Young-Sun Kweon: nillilia01@empas.com; Kyung-Eun Lee: kyuong84@naver.com; Jiyeon Ko: aitt20c@naver.com; Jan C-C. Hu: janhu@umich.edu; James P. Simmer: jsimmer@umich.edu; Jung-Wook Kim: pedoman@snu.ac.kr

[1]Department of Pediatric Dentistry & Dental Research Institute School of Dentistry, Seoul National University, Seoul, Korea 275-1 Yongon-dong, Chongno-gu, Seoul 110-768, Korea

[2]Department of Biologic and Materials Sciences University of Michigan Dental Research Lab 1210 Eisenhower Place, Ann Arbor, MI 48108

[3]Department of Molecular Genetics & Dental Research Institute School of Dentistry, Seoul National University, Seoul, Korea 275-1 Yongon-dong, Chongno-gu, Seoul 110-768, Korea

Abstract

Objective—The aim of this study was to determine if FAM83H over-expression causes dentin or enamel malformations.

Materials and Methods—The full-length mouse *Fam83h* cDNA was inserted into the pCAGIG vector between a β-actin promoter and β-globin enhancer for ubiquitous expression in transgenic mice. Recombinant mouse FAM83H was expressed and used to generate polyclonal antibodies. Western blots showed enhanced expression of the *Fam83h* transgene. The effects of transgene expression on tooth development were assessed by microhardness measurements of enamel and dentin. Total thickness of incisor enamel at the level of the alveolar crest was measured and decussating rod patterns were visualized by scanning electron microscopy (SEM).

Results—Three transgenic mouse lines were selected based upon their transgene expression levels. There was no statistically significant difference in the Vickers microhardness values of enamel or dentin between the transgenic lines or between the transgenic lines and wild type mice. No statistically significant differences in enamel thickness were observed between the transgenic lines and the wild type mice. SEM analysis revealed no apparent differences in the enamel crystal and rod morphologies.

Conclusion—Our findings demonstrate that over-expression of FAM83H in mice does not produce a phenotype in dentin or enamel.

*Corresponding authors: Dr. James P. Simmer, Department of Biologic and Materials Sciences, University of Michigan Dental Research Lab, 1210 Eisenhower Place, Ann Arbor, MI 48108, Tel: 734-975-9315, Fax: 734-975-9329, jsimmer@umich.edu. Dr. Jung-Wook Kim. Department of Molecular Genetics, Department of Pediatric Dentistry & Dental Research Institute, School of Dentistry, Seoul National University, 275-1 Yongon-dong, Chongno-gu, Seoul 110-768, Korea., Tel: +82-2-2072-2639, Fax: +82-2-744-3599 pedoman@snu.ac.kr.

All authors declare there are no competing interests.

Keywords

Amelogenesis imperfecta; dentinogenesis; tooth; Family with sequence similary 83; member h

Introduction

Family with sequence similary 83, member h (*FAM83H*) is an obscure gene and protein that became especially interesting to dentists and scientists studying tooth development when it was discovered that two nonsense mutations (p.Arg325* and p.Gln398*) in *FAM83H* on chromosome 8q24.3 caused autosomal-dominant hypocalcified amelogenesis imperfecta (ADHCAI, OMIM #130900) in humans (1). Additional reports of *FAM83H* mutations causing ADHCAI quickly followed. As of this writing 20 novel *FAM83H* mutations causing ADHCAI have been reported in 33 AI kindreds (Table 1). Six of the *FAM83H* mutations have been identified independently in multiple kindreds.

Amelogenesis imperfecta (AI) is a collection of inherited diseases that exhibit enamel malformations without symptoms outside of the dentition (2). Defects in other genes besides *FAM83H* that have been shown to cause non-syndromic amelogenesis imperfecta include *AMELX* (3), *ENAM* (4), *MMP20* (5), *KLK4* (6), *WDR72* (7), and *C4orf26* (8). Combined, these genes account for about half of all non-syndromic AI cases (9). The other causative genes are unknown.

Defects in *FAM83H* account for more AI cases than any other single gene. *FAM83H* has the most (20) reported novel disease-causing mutations. The number of novel mutations in the other AI-associated genes are: 18 in *AMELX* (10), 12 *ENAM* (11), 5 *C4orf26* (8), 5 *WDR72*, 4 *MMP20*, and 1 *KLK4. FAM83H* mutations are also highest on a percentage basis. Among the 19 AI-causing defects identified in 39 families, 9 were in *FAM83H*, 4 in *ENAM*, 4 in *AMELX*, 2 in *MMP20*, and one in *WDR72* (9).

Despite the relatively high prevalence of AI cases caused by *FAM83H* defects, the FAM83H gene and protein, and the types of mutations that cause disease are both unusual. Unlike most of the genes that cause isolated AI, *FAM83H* does not encode a secreted protein. FAM83H is a cytosolic protein that appears to be associated with the trans-Golgi network (12). Its function in dental enamel formation is unknown. FAM83H expression is not tooth-specific, although it is expressed in developing teeth (13). There are 50 human *FAM83H* expressed sequence tags (ESTs) for normal tissues (which does not include developing teeth) listed in the NCBI database (Hs.67776). The highest levels of FAM83H ESTs are observed in larynx, cervix, and bladder, although no defects in these tissues have been reported in any persons with ADHCAI caused by *FAM83H* mutations. *Fam83h* knockout mice have not yet been characterized.

The intriguing pattern of the 20 AI-causing *FAM83H* mutations is that they are all either nonsense or frameshift mutations in the last coding exon (exon 5) that would truncate the protein (normally 1179 amino acids), but never before Ser^{287} or after Glu^{694}. FAM83H contains an N-terminal phospholipase D-like domain (cd09188) that extends from amino acid 17 to 281. Although recognizable, the homology with phospholipase D is trace and assumed to reflect conservation of its three-dimensional fold, not its catalytic activity. The N-terminal phospholipase D-like domain is the only structural motif shared by the 8 members of the FAM83 group. Among the FAM83H homologues in vertebrates, there is at least a low level of conservation throughout the protein, but the level of identities is exceptionally high from Ser^{149} through Leu^{284} (12). As no ADHCAI-causing truncation mutations have been observed before Ser^{287} or after Glu^{694}, it appears that the condition necessary to cause enamel malformations in humans is expression of an intact N-terminal

phospholipase D-like domain *without* the adjacent functional or regulatory (FvR) domain extending from Ser^{287} to Glu^{694}. Because the adjacent FvR domain bears no homology to any protein of known function, discovering its function will be challenging.

There are several competing hypotheses that might explain the pathological mechanism of FAM83H truncation mutations in a single allele. Previously we truncated mouse FAM83H at four sites homologous to human disease-causing mutations (p.R325*, p.W460*, p.Q677*, p.E964*), which shifted the localization of FAM83H from the cytoplasm to the nucleus in all but p.E964* (14). Perhaps the truncated protein expressed from the mutant *FAM83H* allele translocates to the nucleus, causing pathology. Another hypothesis is that FAM83H functions as a dimer that interacts with other proteins. Base upon phospholipase D crystal structure, dimerization of FAM83H is likely to be mediated by the N-terminal phospholipase D-like domain (15). The FvR domain on both members of the dimer is apparently necessary for proper functioning of FAM83H in developing teeth. The wild-type/truncated heterodimers might lack function (reducing the amount of functional dimers to ¼ normal levels) or dis-regulate FAM83H interacting protein(s) causing pathology through dominant negative or gain of function mechanisms.

The hypothesis that the truncations cause a simple loss of function (reducing the amount of functional protein to ½ normal levels) seems highly unlikely because of the absence of disease-causing missense mutations in critical amino acid positions and the absence of 5′ nonsense, splice junction, or frameshift mutations that would likely induce nonsense mediated decay of the mutant transcripts. These types of defects must occur, but have not been observed in ADHCAI patients. The compelling explanation for this is that such mutations do not cause enamel malformations. Thus haploinsufficiency (under-expression) and simple loss of function are unlikely pathological mechanisms in the etiology of ADHCAI. In this study we test the hypothesis that over-expression of FAM83H causes dental (dentin or enamel) malformations.

Materials and Methods

Protocol approval

The animal protocols were reviewed and approved by the Seoul National University Institutional Animal Care and Use Committee. Experiments were carried out in accordance with the Guidelines established by the National Institute of Health (NIH) regarding the care and use of animals for experimental procedures.

Cloning the Fam83h transgene

Total RNA was isolated from a developing mandible of new born C57BL/6N mouse using Trizol reagent (Invitrogen, Carlsbad, CA) as described. First strand cDNA was made using oligo$(dT)_{18}$ primer with Transcriptor First Strand cDNA synthesis kit (Roche, Mannheim, Germany) according to the manufacturer's instructions. *Fam83h* coding sequence was amplified (sense primer: 5′-tgaattCTGGCCCCAAC**ATG**GCCCGT, antisense primer: 5′-tgcggccgcTCCGAGACCAGGAGATCATT). The amplified product was cloned into the pCAGIG vector (Addgene plasmid 11159, Addgene, Cambridge, MA) (16) after digestion with *Eco*RI and *Not*I restriction endonucleases. Correct clone was selected and confirmed by direct sequencing. The pCAGIG vector combines the chicken β-actin ubiquitous high promoter activity with a rabbit β-globin gene enhancer (17).

Generation of Fam83h transgenic mice

The 8.0-kb *Fam83h* transgene was excised from the vector by double digestion with *Sal*I and *Drd*I restriction endonucleases and used to generate Fam83h transgenic C57BL/6N mice

(Macrogen, Seoul, Korea). A total of 13 independent lines were generated and mated with C57BL/6 mice. Germline transmission was determined by PCR analysis of genomic DNA isolated from tail biopsies (sense primer: 5′-CTCTAGAGCCTCTGCTAACCA, antisense primer: 5′-ACACGCAGGAAGTCCACATGA).

Generation of Fam83h polyclonal antibody

Full length *Fam83h* coding region was cloned into pET-3a vector (Novagen, Madison, WI) using *Nde*I and *Bam*HI double digestion after PCR amplification (sense primer: 5′-cgccatATGGCCCGTCGCTCCCAGAGCAGCT, antisense primer: 5′-gggatcctgCTTCTCC TTTAGATGGCCCTTGA). Expressed protein was excised from the gel and used to generate a rabbit polyclonal antibody (AbFrontier, Seoul, Korea).

Transgene expression assessment by Western blotting

Ten lines with germline transmission were tested for the transgene expression by Western blot analyses. Protein was isolated from tail cutting using a mortar and pestle with liquid nitrogen and RIPA buffer (ElpisBio, Taejeon, Korea) and centrifuged. The extract was fractionated by SDS-PAGE on a 7% Tris–glycine gel, transblotted onto a Hybond-ECL membrane (GE Healthcare Bio-Sciences, Piscataway, NJ, USA), incubated with blocking solution, immunostained using the primary antibody 1:3000 at 4°C overnight and the secondary antibody anti-rabbit (Abcam, Cambridge, MA, USA) 1:8000 at room temperature for 1 hr. Transgenic mice with the highest expression of FAM83H were selected for further characterization.

Microhardness measurement of enamel and dentin

Finally three lines were selected based upon the transgene expression level. A total of 27 transgenic mice (TG1; 8, TG2; 8, TG3; 11) and ten wild type mice were sacrified and their mandibles collected. The isolated mandibles were embedded in polyacrylic resin. The mandibles were sectioned through the incisors at the level of the alveolar crest and polished using a series of SiC papers (220, 600, 800, 1000, 2000 and 4000 grit). The microhardness score was measured at six points in the center mesial-distally on the incisor cross-sections, (enamel; near surface, middle, near DEJ, dentin; near DEJ, middle, near pulpal) (Fig. 1). This position was selected because the incisors are in late maturation stage, but still in the unerupted portion where they have not been affected by occlusal forces. The measurements of the microhardness were repeated three times and averaged at each point. Vickers microhardness (VHN) was measured using a microhardness tester (HMV-2, Schimadzu, Tokyo, Japan) where a 490.3mN load was applied for five seconds to obtain the measurement.

Measurement of the enamel thickness

Enamel thickness was measured from the DEJ to the outer enamel surface on the line perpendicular to the outer enamel surface at its thickest point was measured three times using HMV-2 and averaged.

Scanning Electron Microscopy (SEM) of mandibular incisors

Specimens were etched with 37% phosphoric acid for ten seconds and washed with copious water for 20 s. Specimen surfaces were sputter-coated with carbon after drying and analyzed with SEM (Hitachi, S4700, Tokyo, Japan) under 15 KV condition.

Results

Three transgenic lines were selected based upon germline transmission and the expression level of transgene (TG1, TG2 and TG3) (Fig. 2). There was no statistically significant difference in the Vickers microhardness value of the enamel and dentin between the transgenic lines (TG1, TG2 and TG3) (one way ANOVA, $p>0.05$) (Table 2). The microhardness values of the three lines were combined and compared to those of wild type mice. Statistical analysis showed no difference between the trangenic mice and wild type mice in their enamel and dentin microhardness values (student's t-test, $p>0.05$) (Table 3). Likewise there was no statistically significant differences in enamel thickness (Table 4), and no apparent differences in the enamel crystal and rod morphologies, between the transgenic lines and the wild type mice (Fig. 3).

Discussion

Among the genes currently known to cause isolated amelogenesis imperfecta, only two (*FAM83H* and *ENAM*) show an autosomal dominant pattern of inheritance. Roughly 2/3 of autosomal dominant AI cases are caused by these two genes (9). An ADHCAI proband with enamel malformations similar to those caused by defects in *FAM83H* showed no putative disease-causing mutations in the *FAM83H* coding exons or intron borders (18). Possibly FAM83H interacts with the product of that unknown gene and a loss of function of the interacting complex causes the distinctive ADHCAI enamel phenotype.

Because FAM83H disease-causing mutations are restricted to those that truncate the protein within a specific segment of exon 5, it seems clear that simple haploinsufficiency (50% expression level of the wild type protein) does not produce a phenotype. In this study we show that over-expression of FAM83H in mice does not produce a phenotype. Taken together, enamel defects do not appear to be caused by variations in FAM83H expression levels within the range of 50% to ~400% of normal (50% because haploinsufficiency does not cause an enamel phenotype in humans; ~400% from the absence of a phenotype in over-expressing mice). The mouse findings support the conclusion that *FAM83H* mutations cause ADHCAI through a dominant negative or gain of function mechanism, rather than through changes in FAM83H expression levels. It follows that the ADHCAI-causing nonsense and frameshift alleles in exon 5 of *FAM83H* express viable RNA transcripts that escape the nonsense-mediated decay (NMD) pathway and are translated to generate a truncated protein. This is consistent with previous observations that premature translation termination codons in the last coding exon generally escape nonsense-mediated decay (19).

Other inherited diseases besides ADHCAI are associated specifically with truncation mutations. Particularly interesting are the cases of SRY related homeobox gene 10 (*SOX10*) and myelin protein-zero (*MPZ*) mutations (20). Most disease-associated mutations in the *SOX10* transcription factor gene result in premature termination codons. Such mutations cause two distinct phenotypes: the more severe PCWH syndrome (OMIM 609136), which is an acronym for the four syndromes combined in its phenotype, and the milder Waardenburg-Shah syndrome (OMIM 277580). The severe and mild forms are both caused by nonsense and frameshift mutations. PCWH syndrome is caused by dominant-negative activity of the truncated protein (as appears to be the case for ADHCAI caused by *FAM83H* defects), while Waardenburg-Shah syndrome is caused by haploinsufficiency due to degradation of the mutant mRNAs by the nonsense-mediated decay pathway. Triggering or escaping NMD determines the phenotype.

Myelin protein-zero is the major structural protein of peripheral myelin. *MPZ* has six exons. Mutations in the early exons induce NMD, causing haploinsufficiency and a milder clinical

phenotype, as in Charcot-Marie-Tooth disease (OMIM 118200). Mutations in the last exon escape NMD and are associated with Dejerine-Sottas syndrome (OMIM 145900), which has a more severe phenotype that is caused by accumulation of the truncated protein in the endoplasmic reticulum followed by apoptosis (21).

FAM83H mutations fall into a similar pattern, except there is no milder form of the disease because haploinsufficiency doesn't produce a recognizable phenotype. Transcripts degraded by NMD do not cause disease. Curiously, a single nucleotide deletion identified in the last exon of dog *Fam83h* showed no discernable phenotype in heterozygotes, even though the frameshift is similar to those that cause ADHCAI in humans (22). Perhaps NMD degrades the mutation transcript in dogs. Enamel malformations were not even observed in the homozygous mutants, although the dogs suffered from congenital keratoconjunctivitis sicca and ichthyosiform dermatosis. This raises the possibility that FAM83H may not be critical for tooth formation, but cells in human developing teeth are particularly susceptable to the dominant negative or gain of function effects of expression of the truncated protein. It will be interesting to see if a total absence of *FAM83H* expression causes an enamel phenotype in *Fam83h* null mice.

Acknowledgments

This work was supported by grants from the Bio & Medical Technology Development Program (2011-0027790), the Science Research Center grant to Bone Metabolism Research Center (2012-0000487) by the Korea Research Foundation Grant (KRF-2008-313-E00597) funded by the Korean Ministry of Education, Science and Technology and by NIDCR/NIH Grant DE019622.

References

1. Kim JW, Lee SK, Lee ZH, Park JC, Lee KE, Lee MH, et al. FAM83H mutations in families with autosomal-dominant hypocalcified amelogenesis imperfecta. American Journal of Human Genetics. 2008; 82:489–94. [PubMed: 18252228]
2. Witkop CJ Jr. Amelogenesis imperfecta, dentinogenesis imperfecta and dentin dysplasia revisited: problems in classification. Journal of Oral Pathology. 1989; 17:547–53. [PubMed: 3150442]
3. Lagerström M, Dahl N, Nakahori Y, Nakagome Y, Backman B, Landegren U, et al. A deletion in the amelogenin gene (AMG) causes X-linked amelogenesis imperfecta (AIH1). Genomics. 1991; 10:971–5. [PubMed: 1916828]
4. Rajpar MH, Harley K, Laing C, Davies RM, Dixon MJ. Mutation of the gene encoding the enamel-specific protein, enamelin, causes autosomal-dominant amelogenesis imperfecta. Human Molecular Genetics. 2001; 10:1673–7. [PubMed: 11487571]
5. Kim JW, Simmer JP, Hart TC, Hart PS, Ramaswami MD, Bartlett JD, et al. MMP-20 mutation in autosomal recessive pigmented hypomaturation amelogenesis imperfecta. Journal of Medical Genetics. 2005; 42:271–5. [PubMed: 15744043]
6. Hart PS, Hart TC, Michalec MD, Ryu OH, Simmons D, Hong S, et al. Mutation in kallikrein 4 causes autosomal recessive hypomaturation amelogenesis imperfecta. Journal of Medical Genetics. 2004; 41:545–9. [PubMed: 15235027]
7. El-Sayed W, Parry DA, Shore RC, Ahmed M, Jafri H, Rashid Y, et al. Mutations in the beta propeller WDR72 cause autosomal-recessive hypomaturation amelogenesis imperfecta. American Journal of Human Genetics. 2009; 85:699–705. [PubMed: 19853237]
8. Parry DA, Brookes SJ, Logan CV, Poulter JA, El-Sayed W, Al-Bahlani S, et al. Mutations in C4orf26, encoding a peptide with in vitro hydroxyapatite crystal nucleation and growth activity, cause amelogenesis imperfecta. American Journal of Human Genetics. 2012; 91:565–71. [PubMed: 22901946]
9. Chan HC, Estrella NM, Milkovich RN, Kim JW, Simmer JP, Hu JC. Target gene analyses of 39 amelogenesis imperfecta kindreds. European Journal of Oral Sciences. 2011; 119:311–23. [PubMed: 22243262]

10. Hu JC-C, Chan H-C, Simmer SG, Seymen F, Richardson AS, Hu Y, et al. Amelogenesis imperfecta in two families with defined AMELX deletions in ARHGAP6. PLoS One. 2012; 7:e52052. [PubMed: 23251683]
11. Simmer S, Estrella N, Milkovich R, Hu J. Autosomal dominant amelogenesis imperfecta associated with ENAM frameshift mutation p. Asn36Ilefs56. Clinical Genetics. 2012; 29:1–3.
12. Ding Y, Estrella MR, Hu YY, Chan HL, Zhang HD, Kim JW, et al. Fam83h is associated with intracellular vesicles and ADHCAI. Journal of Dental Research. 2009; 88:991–6. [PubMed: 19828885]
13. Lee MJ, Lee SK, Lee KE, Kang HY, Jung HS, Kim JW. Expression patterns of the Fam83h gene during murine tooth development. Archives of Oral Biology. 2009; 54:846–50. [PubMed: 19545854]
14. Lee SK, Lee KE, Jeong TS, Hwang YH, Kim S, Hu JC, et al. FAM83H Mutations Cause ADHCAI and Alter Intracellular Protein Localization. Journal of Dental Research. 2011; 89:1378–82. [PubMed: 20938048]
15. Stuckey JA, Dixon JE. Crystal structure of a phospholipase D family member. Nature Structural & Molecular Biology. 1999; 6:278–84.
16. Matsuda T, Cepko CL. Electroporation and RNA interference in the rodent retina in vivo and in vitro. Proceedings of the National Academy of Sciences of the United States of America. 2004; 101:16–22. [PubMed: 14603031]
17. Miyazaki J, Takaki S, Araki K, Tashiro F, Tominaga A, Takatsu K, et al. Expression vector system based on the chicken beta-actin promoter directs efficient production of interleukin-5. Gene. 1989; 79:269–77. [PubMed: 2551778]
18. Song YL, Wang CN, Zhang CZ, Yang K, Bian Z. Molecular characterization of amelogenesis imperfecta in Chinese patients. Cells Tissues Organs. 2012; 196:271–9. [PubMed: 22414746]
19. Shyu AB, Wilkinson MF, van Hoof A. Messenger RNA regulation: to translate or to degrade. The EMBO Journal. 2008; 27:471–81. [PubMed: 18256698]
20. Inoue K, Khajavi M, Ohyama T, Hirabayashi S, Wilson J, Reggin JD, et al. Molecular mechanism for distinct neurological phenotypes conveyed by allelic truncating mutations. Nature Genetics. 2004; 36:361–9. [PubMed: 15004559]
21. Khajavi M, Inoue K, Wiszniewski W, Ohyama T, Snipes GJ, Lupski JR. Curcumin treatment abrogates endoplasmic reticulum retention and aggregation-induced apoptosis associated with neuropathy-causing myelin protein zero-truncating mutants. American Journal of Human Genetics. 2005; 77:841–50. [PubMed: 16252242]
22. Forman OP, Penderis J, Hartley C, Hayward LJ, Ricketts SL, Mellersh CS. Parallel mapping and simultaneous sequencing reveals deletions in BCAN and FAM83H associated with discrete inherited disorders in a domestic dog breed. PLoS Genetics. 2012; 8:e1002462. [PubMed: 22253609]
23. Wright JT, Frazier-Bowers S, Simmons D, Alexander K, Crawford P, Han ST, et al. Phenotypic variation in FAM83H-associated amelogenesis imperfecta. Journal of Dental Research. 2009; 88:356–60. [PubMed: 19407157]
24. Lee SK, Hu JC-C, Bartlett JD, Lee KE, Lin BP-J, Simmer JP, et al. Mutational spectrum of FAM83H: The C-terminal portion is required for tooth enamel calcification. Human Mutation. 2008; 29:E95–E9. [PubMed: 18484629]
25. Haubek D, Gjorup H, Jensen LG, Juncker I, Nyegaard M, Borglum AD, et al. Limited phenotypic variation of hypocalcified amelogenesis imperfecta in a Danish five-generation family with a novel FAM83H nonsense mutation. International Journal of Paediatric Dentistry. 2011; 21:407–12. [PubMed: 21702852]
26. Hart PS, Becerik S, Cogulu D, Emingil G, Ozdemir-Ozenen D, Han ST, et al. Novel FAM83H mutations in Turkish families with autosomal dominant hypocalcified amelogenesis imperfecta. Clinical Genetics. 2009; 75:401–4. [PubMed: 19220331]
27. Wright JT, Torain M, Long K, Seow K, Crawford P, Aldred MJ, et al. Amelogenesis imperfecta: genotype-phenotype studies in 71 families. Cells Tissues Organs. 2011; 194:279–83. [PubMed: 21597265]

28. Hyun HK, Lee SK, Lee KE, Kang HY, Kim EJ, Choung PH, et al. Identification of a novel FAM83H mutation and microhardness of an affected molar in autosomal dominant hypocalcified amelogenesis imperfecta. International Endodontic Journal. 2009; 42:1039–43. [PubMed: 19825039]

29. El-Sayed W, Shore RC, Parry DA, Inglehearn CF, Mighell AJ. Ultrastructural analyses of deciduous teeth affected by hypocalcified amelogenesis imperfecta from a family with a novel Y458X FAM83H nonsense mutation. Cells Tissues Organs. 2010; 191:235–9. [PubMed: 20160442]

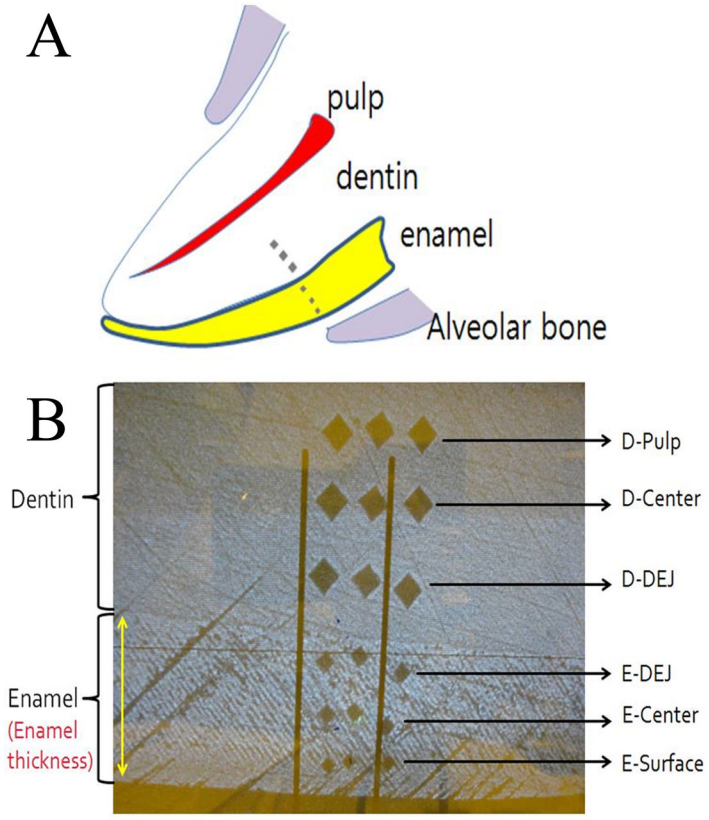

Figure 1.
(A) Illustration of the mouse incisor showing the site used for indentation. (B) HMV-2 (magnifications 40x) image showing indentation positions used for the Vickers microhardness testing of mouse incisor enamel and dentin. The indentations were made perpendicular to the enamel surface above the end of the alveolar bone. Key: E-surface, point in the enamel near the enamel surface; E-center ; point in the enamel between the E-surface and E-DEJ; E-DEJ ; point in the enamel near the DEJ; D-DEJ ; point in the dentin near the DEJ; D-center ; point in the dentin between the D-DEJ and D-pulp; D-pulp ; point in the dentin near the pulp.

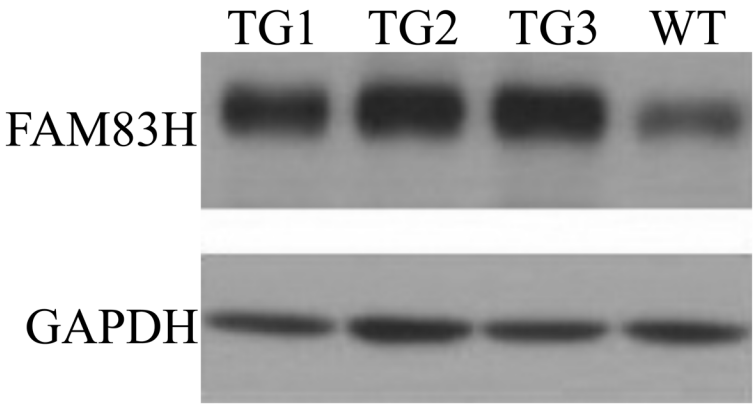

Figure 2.
Western blot using the tooth protein extracts of the transgenic and wild type mice. Expression of *Fam83h* in the transgenic mice is higher than in the wild type mice. Degree of expression increased from the wild type (lowest expression) to TG1, to TG2, and was highest in TG3. We estimated FAM83H expression to be at least 4x greater than normal.

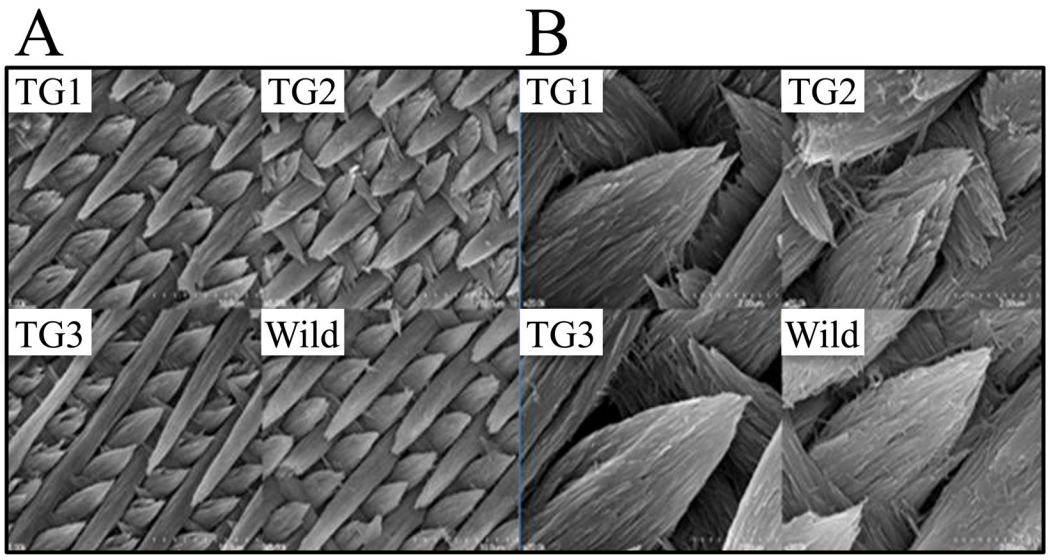

Figure 3.
Scanning electron microscopy (SEM) of enamel. There is no apparent difference in the structure of the enamel crystal and rod between each group. (A) Magnifications of 5000x. (B) Magnification is 20000x. The images show maturation stage enamel rods located near the center of the enamel layer (both mesial-distally and from the DEJ to the enamel surface).

Table 1

Sites of *FAM83H* mutations causing ADHCAI. FAM83H primary sequence showing the positions of the 20 novel AI-causing *FAM83H* nonsense (bold) or frameshift (bold/italic) mutations. The cDNA numbers in the mutation list start from the translation initiation site of *FAM83H* reference sequence NM_198488.3.

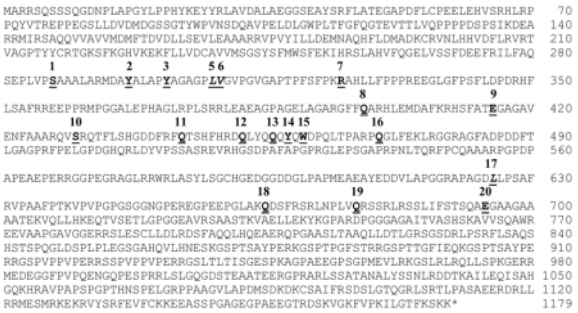

#	cDNA	Protein	References
1	c.860C>A	p.S287*	(23)
2	c.891T>A	p.Y297*	(24)
3	c.906T>G	p.Y302*	(18, 25)
4	c.923_924delTC	p.L308fs*323	(23)
5	c.924dupT	p.V309Rfs*324	(18)
6	c.973C>T	p.R325*	(1, 18)
7	c.1192C>T	p.Q398*	(1, 26) (12, 27)
8	c.1243G>T	p.E415*	(24)
9	c.1289C>A	p.S430*	(27)
10	c.1330C>T	p.Q444*	(12, 26)
11	c.1354C>T	pQ452*	(25, 28) (9, 18)
12	c.1366C>T	p.Q456*	(26)
13	c.1374C>A	p.Y458*	(29)
14	c.1379G>A	p.W460*	(23)
15	c.1380G>A	p.W460*	(24)
16	c.1408C>T	p.Q470*	(23)
17	c.1872_1873delCC	p.L625fs*703	(23)
18	c.1993 C>T	p.Q665*	(14)
19	c.2029 C>T	p.Q677*	(14, 24) (9, 18, 27)
20	c.2080G>T	p.E694*	(23)

Table 2

Comparison of Vickers microhardness numbers between TG1, TG2, and TG3 using one way ANOVA

	TG1(N=8)	TG2(N=8)	TG3(N=11)		
	mean±SD	mean±SD	mean±SD	F	*P*-value
E-surface	266.83±14.63	260.03±15.86	268.49±14.34	0.78	0.46
E-center	221.88±20.71	226.58±12.29	223.73±13.30	0.19	0.83
E-DEJ	198.08±19.57	203.46±11.04	200.64±12.79	0.27	0.76
D-DEJ	82.05 ± 2.81	81.98 ± 2.97	81.73 ± 2.83	0.03	0.96
D-center	77.48 ± 3.06	77.15 ± 4.39	78.59 ± 3.54	0.41	0.66
D-pulp	76.40 ± 3.94	75.15 ± 4.22	76.09 ± 3.97	0.21	0.81

Table 3

Means of the Vickers microhardness numbers of wild type and transgenic mice incisors.

		TG(N=27)	Wild type(N=10)	
		mean±SD	mean±SD	*P*-value
Enamel	E-Surface	265.51±14.76	269.77±13.03	0.43
	E-Center	224.03±15.09	219.90±16.40	0.47
	E-DEJ	200.72±14.26	198.63±12.46	0.68
Dentin	D-DEJ	81.90± 2.76	81.60± 3.78	0.79
	D-Center	77.84± 3.60	77.93± 3.32	0.94
	D-Pulp	75.90± 3.91	75.03± 2.95	0.52

*TG = TG1 + TG2 + TG3

Table 4

Comparison of the enamel thickness between each group using one way ANOVA.

	N	Mean±SD(μm)	F	*P*-value
TG1	8	202.00±17.20	0.26	0.85
TG2	8	196.75±14.80		
TG3	11	201.36±20.99		
Wild	10	207.10±37.63		
Total	37	202.05±24.29		